JOURNAL OF SOLID STATE CHEMISTRY 87, 264–273 (1990)

Potassium Ferrites of $KFeO_2$ and $K_{1+x}Fe_{11}O_{17}$ Systems ($x = 0$–1): Studies on Leaching Behavior in Fused Iron Catalysts

LI FAN, WANG WEN-XIANG, HAN QI-KUN, AND WANG LING

Chemistry Department of Zhengzhou University, Zhengzhou, Henan, People's Republic of China

Received June 28, 1989; in revised form February 5, 1990

Two series of potassium ferrites, $KFeO_2$ and $K_{1+x}Fe_{11}O_{17}$ ($x = 0$–1), were prepared by several methods and their leaching process was studied. Because of its structural characteristics, $KFeO_2$ can be easily hydrolyzed and its structure can be completely destroyed during leaching in water, whereas for $K_{1+x}Fe_{11}O_{17}$ only a portion of the potassium ions shifts out of the system and its structure still remains after soaking in water. The kinetic parameters for potassium leaching from the $K_{1+x}Fe_{11}O_{17}$ system have also been determined. It is suggested that both types of potassium ferrites coexist in fused iron catalysts for ammonia synthesis: $KFeO_2$ occurs at boundaries, while $K_{1+x}Fe_{11}O_{17}$ mainly remains in the crystal grains of the catalyst. The former belongs to the so-called soluble and the latter to the insoluble potash of the catalyst. The catalytic activity largely depends on the latter.

Introduction

Since the beginning of this century when Haber and Bosch developed a practical process for ammonia synthesis, fused iron catalysts have been of industrial and theoretical importance. These iron catalysts are still in use today; such promoters as K_2O, Al_2O_3, and CaO are varied according to industrial demand, and other oxides, such as, some rare-earth oxides and cobalt oxide, are often added. It is very important to understand the forms, properties, and roles of promoters which, although introduced in small amounts, greatly improve the function of the catalysts.

The promotional action of potassium is generally ascribed to its acceleration of dissociative nitrogen adsorption due to a lowering of the local work function. Recent results issued by Paál *et al.* (*1*) showed that a composite Fe–O–K adlayer is probably the actual surface phase under operating conditions of the iron catalyst (when iron is in the reduced state), rather than any known bulk potassium compound. The catalytic properties of potassium are still more controversial than those of Al_2O_3 (*2*, *3*), particularly its chemical state in the unreduced catalyst.

Nielsen (*4*) presented electron microprobe results of a triply promoted catalyst (K_2O–Al_2O_3–CaO) in the unreduced state, in which potassium occurs mainly at the grain boundaries of the unreduced magnetite. Modern surface spectroscopic techniques have provided many new approaches for exploring the microscopic structure of the catalyst (*5*, *6*). An XPS study on the chemical nature and compositions of the surfaces of the fused iron catalyst was carried out by Ertl and Thiele (*6*). They encountered a strong enrichment

0021-9517/90 $3.00

of K and Al at the surface of the unreduced catalyst. On the other hand, Kobayashi and Nishijima (*7*) indicated that the potash existing in the unreduced catalyst could be divided into two components, a part soluble in water and a part insoluble in water, and that the larger the content of the latter, the greater the activity for ammonia synthesis. Later Uchida and Todo (*8*) concluded from electronic images that there are three kinds of potash-rich regions, i.e., grain boundaries, particularly interfacial grains, and some subgrains into which the parent grains are divided. They believed that potash in the subgrains is probably insoluble in water and contributes most to the activity for the ammonia synthesis as described by Kobayashi. In our previous work, it was also noted that insoluble K exists in the unreduced catalyst, despite the high concentration of K at the surface (*9*). Therefore, it is still an outstanding problem to determine the chemical composition of the insoluble potash and to determine the reason for its insolubility in water.

On the other hand, two series of potassium ferrite with different structures, $KFeO_2$ and $K_{1+x}Fe_{11}O_{17}$ (x = 0–1), have been studied. Tomkowizc and Szytuka (*10*) reported on the preparation of potassium ferrite of the $KFeO_2$ type and determined its crystal and magnetic structure by neutron and X-ray diffraction and Mössbauer spectroscopy. In addition, the properties of the potassium ferrite of the $K_{1+x}Fe_{11}O_{17}$ type (x = 0–1), among which the more typical compounds are $K_2Fe_{12}O_{19}$ (x = 0.83), $K_2Fe_{14}O_{22}$ (x = 0.57), and $K_2Fe_{22}O_{34}$ (x = 0), have been described elsewhere in detail (*11–13*). However, we found no report in the literature on these two systems as promoters of the fused iron catalyst for ammonia synthesis.

In this paper we report on the preparation of two types of potassium ferrite under conditions similar to those for the production of the fused iron catalyst. We also report the kinetics of leaching out potassium in an attempt to correlate these with soluble and insoluble potash as promoters in the fused iron catalyst.

Experimental

1. Preparation of Samples

According to the methods described in the literature (*10–13*), both types of potassium ferrite can be prepared by calcinating K_2CO_3 or KNO_3 together with Fe_2O_3 at 800, 1000, or 1200°C in several stages while not exceeding 1300°C. In our studies, KNO_3, Fe_3O_4, K_2CO_3, and α-Fe_2O_3 were employed as starting materials and calcined in a corundum crucible above 1500°C in order to follow the preparation condition under which the typical commercial catalyst for ammonia synthesis is produced.

The following samples were prepared:

Sample A: a mixture of α-Fe_2O_3 and K_2CO_3 with a molar ratio of 1 : 1 was heated to 1000°C in 2 hr and maintained at this temperature for 0.5 hr.

Sample B: a mixture of Fe_3O_4 and K_2CO_3 in an atomic ratio of K : Fe = 1 : 1 was heated following the procedure used for sample A.

Samples C, D, and E: α-Fe_2O_3 and K_2CO_3 with atomic ratios of K : Fe = 1 : 11, 1 : 7, and 1 : 6 for samples C, D, and E, respectively, were ground and pressed into tablets. They were calcined as follows: For sample C, tablets were maintained at 1100°C for 1 hr. The product was crushed and heated again in the form of tablets at 1300°C for 5 hr, then rapidly cooled to room temperature. For sample D, the tablets were heated at 800°C for 1 hr. After cooling, the product was heated again in the form of tablets at 800°C for 3 hr, at 1000°C for 1 hr, and at 1200°C for 3 hr; then it was cooled slowly to room temperature. For sample E, the first calcinating

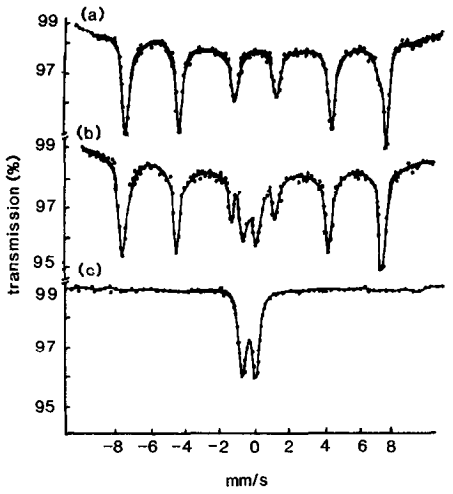

FIG. 1. Mössbauer spectra of $KFeO_2$: (a) when fresh, (b) exposed for a time in air, (c) exposed in air for 24 hr or soaked in water at 70°C for 0.5 hr.

temperature was also 800°C for 1 hr, and the second calcinating temperature was 1200°C for 5 hr. The product was rapidly cooled, as for sample C.

For Sample F, the pure magnetite with 10 wt% KNO_3 and 5 wt% pure iron powder (atomic ratio of K : Fe = 1 : 11) was pressed into tablets and calcined in an air-tight crucible at 1550°C for 3 hr. The product was slowly cooled to room temperature.

2. *Soaking Samples in Water*

Each of samples was crushed and sieved to 20–40 mesh, 100–120 mesh, and <200 mesh, respectively. Five grams of the sample was accurately weighed out and transferred to a conical flask with a ground stopper which had been filled with 100 ml of ion-free water. The flask was placed in a thermostated water bath so that the water temperature could be controlled. After the sample had been soaked for a proper time, 2 ml of the water solution in the flask was pipetted out for analysis of K_2O, using a flame photometer.

3. *X-Ray Diffraction and Mössbauer Spectroscopy*

The X-ray diffraction data were recorded on Rigaku-XRD (D/MAX-3B) with Cu$K\alpha$ or Cr$K\alpha$ radiation. The Mössbauer spectra at room temperature were taken from an AME-50 Mössbauer spectrometer using a ^{57}Co source in Pd. An α-Fe foil 25 μm in thickness was used as a standard to calibrate the velocity scale of the spectrometer. The counting rates of the spectra varied between 0.3 and 0.4 $\times$ 10^6 counts per channel. The absorber density was 8 mg of natural Fe/cm^2.

Results and Discussion

1. *$KFeO_2$ before and after Water Treatment*

Figures 1a and 2a show the Mössbauer spectrum and XRD diagram of $KFeO_2$ prepared according to methods A and B, respectively. The Mössbauer parameters obtained by computer fitting of the spectra are listed in Table I. When fresh, samples A and B exhibit the same characteristic magnetic splitting in their Mössbauer spectra and

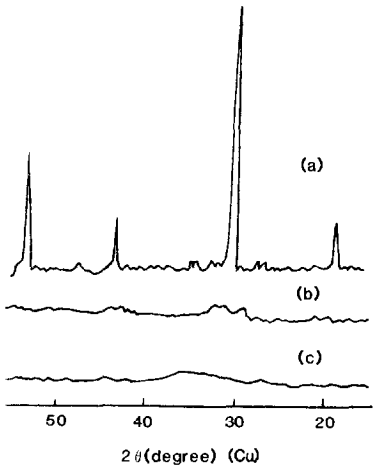

FIG. 2. X-ray diffraction patterns of $KFeO_2$: (a) when fresh, (b) exposed for a time in air, (c) exposed in air for 24 hr or soaked in water at 70°C for 0.5 hr.

TABLE I

MÖSSBAUER PARAMETERS

Sample		IS (mm/sec)	QS (mm/sec)	H (KOe)
$KFeO_2$:	calc.	0.19	0.03	495
	Ref. (*10*)	0.152 ± 0.015	0.037 ± 0.015	501 ± 5
β-FeOOH:	calc.	0.34	0.67	
(small particle)	Ref. (*24*)	0.315 ± 0.025	0.690 ± 0.055	

Note. IS vs α-Fe.

same X-ray diffraction pattern, which are consistent with those reported in Refs. (*10*) and (*14*). These results suggest that Fe_2O_3 or Fe_3O_4 together with K_2CO_3 as starting materials might form potassium ferrite of the $KFeO_2$ type when the atomic ratio of K and Fe is close to 1 : 1. For sample B, the oxidation of Fe_3O_4 to Fe_2O_3 precedes the formation of $KFeO_2$.

A new doublet having an isomer shift (IS) of 0.34 mm/sec and a quadrupole splitting (QS) of 0.67 mm/sec, emerged in the paramagnetic region of the Mössbauer spectra and gradually intensified while the samples were exposed to air. When samples were exposed to air for a sufficiently long time (about 20 hr), the original six characteristic magnetic peaks of $KFeO_2$ were replaced by two paramagnetic peaks. At this point the X-ray diffraction pattern of the samples also disappeared (see Figs. 1b, 1c, 2b, and 2c). When fresh samples were soaked in water at 70°C for 0.5 hr, most of the potassium in them was dissolved into the water; their Mössbauer spectra and X-ray diagrams also showed the same patterns as those in Figs. 1c and 2c. Evidently the fresh potassium ferrite of the $KFeO_2$ type absorbs moisture and is very easily hydrolyzed into amorphous $Fe_2O_3 \cdot xH_2O$ and KOH.

The $KFeO_2$-type potassium ferrite has the same cristobalite structure as that of NaAl SiO_4 (*10, 15, 16*). Each iron ion occupies an equivalent site surrounded by four O^{2-}, composing a tetrahedron. Every potassium ion is in an interstitial position formed by 12 oxygen ions. The interatomic distances in the idealized structure are as follows: O–O = 2.82 Å, Fe–O = 1.73 Å, and K–O = 3.32 Å. The last is larger than the sum of $r_{O^{2-}}$ (= 1.33 Å) and r_{K^+} (= 1.4 Å). Unavoidably, the cristobalite structure of $KFeO_2$ is very loose and the bond between K^+ and O^{2-} is very weak so that it can be readily attacked by water or moisture.

2. *$K_{1+x}Fe_{11}O_{17}$ before and after Water Treatment*

The analyses of K in samples C, D, and E after calcination were consistent with the original chemical mixture, i.e., K : Fe = 1 : 11, 1 : 7 and 1 : 6, respectively. The X-ray diffraction diagrams and the Mössbauer spectra are shown in Figs. 3 and 4, and appear to be similar, in spite of the weak six-line overlapping peaks in the Mössbauer spectrum of sample C, which are ascribed to a small amount of unreacted Fe_2O_3. The XRD diagram is in good agreement with that of $K_2Fe_{22}O_{34}$ indexed in PDF (*14*), and the patterns of the Mössbauer spectra are also reported by Howe and Dudley (*17*).

Potassium ferrite of the $K_{1+x}Fe_{11}O_{17}$ type has the same structure as potassium β-alumina ($K_2O \cdot 11Al_2O_3$) and differs greatly from that of $KFeO_2$. $K_{1+x}Fe_{11}O_{17}$ contains spinel blocks involving four layers of oxygen ions; all iron ions are separated by layers

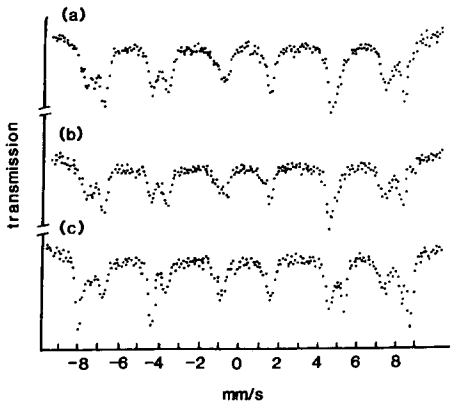

FIG. 3. Mössbauer spectra of the $K_{1+x}Fe_{11}O_{17}$ series before water treatment: (a) $K_2Fe_{12}O_{19}$, (b) $K_2Fe_{14}O_{22}$, (c) $K_2Fe_{22}O_{34}$.

of potassium and oxygen ions. Within the stoichiometric unit cell of $K_2Fe_{22}O_{34}$, iron occupies 12 spinel-type octahedral sites and four spinel-type tetrahedral sites in the layers, as well as two octahedral sites and four tetrahedral sites within the spinel block. The Mössbauer spectrum of $K_{1+x}Fe_{11}O_{17}$ at room temperature was resolved into four six-line hyperfine splittings that were correlated with the four sites, respectively. For $X > 0$, the excess x of potassium ion may be distributed in the mirror plane. The excess potassium ions in the mirror plane of this configuration will not result in a transformation of the spinel blocks and will have little effect on the XRD and MES diagrams of the samples because these ions are relatively free.

In contrast to $KFeO_2$, potassium cannot readily be dissolved out from $K_{1+x}Fe_{11}O_{17}$ by water. Figure 5 shows the percentage of potassium ion dissolved into water at 70°C vs time corresponding to different potassium ferrites. The amount of K_2O derived from $K_{1+x}Fe_{11}O_{17}$ is less than 35% of the total content, even when the samples were ground to 200 mesh and soaked in water for 48 hr at 90°C. It is particularly noteworthy that there are relatively few visual changes

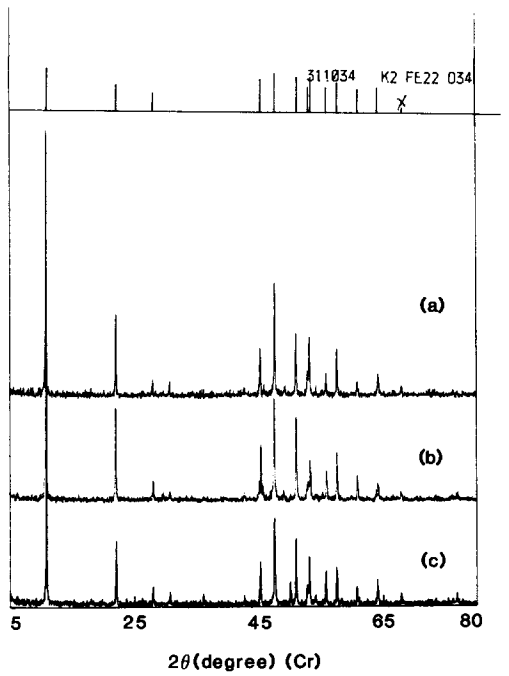

FIG. 4. X-ray diffraction of the $K_{1+x}Fe_{11}O_{17}$ series before water treatment: (a) $K_2Fe_{12}O_{19}$. (b) $K_2Fe_{14}O_{22}$, (c) $K_2Fe_{22}O_{34}$.

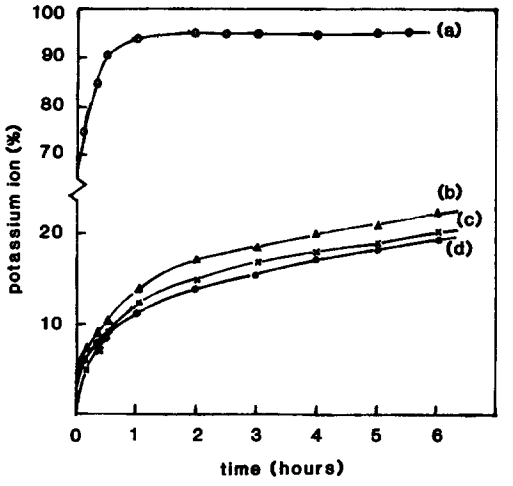

FIG. 5. Plots of percentage of potassium ion dissolved out into water at 70°C versus time: (a) $KFeO_2$, (b) $K_2Fe_{22}O_{34}$, (c) $K_2Fe_{14}O_{22}$, (d) $K_2Fe_{12}O_{19}$ (the size of samples is below 200 mesh).

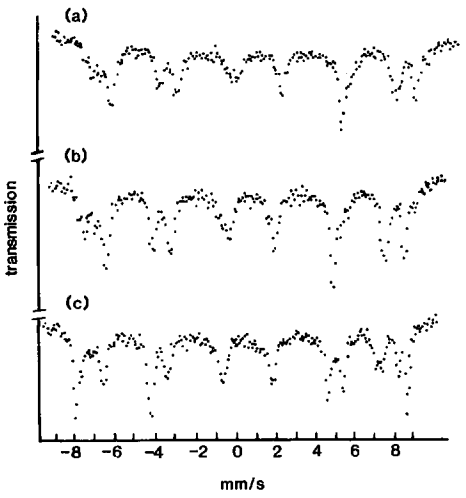

FIG. 6. Mössbauer spectra of $K_{1+x}Fe_{11}O_{17}$ series after having been soaked in water at 90°C for 48 hr: (a) $K_2Fe_{12}O_{19}$, (b) $K_2Fe_{14}O_{22}$, (c) $K_2Fe_{22}O_{34}$.

in the MES and XRD diagrams of the samples after they have been soaked in water (see Fig. 6), suggesting that the removal of potassium from phases of $K_{1+x}Fe_{11}O_{17}$ has very little effect on their structure.

The different stability of the two types of potassium ferrites in water can be attributed to their individual structures. In $K_{1+x}Fe_{11}O_{17}$, the K ions are enclosed by the spinel cells composed of Fe^{3+} and O^{2-} and the spinel blocks are relatively firmer. It is then difficult to shift K^+ out from the solid phase, and the β-alumina structure remains fundamentally intact, whereas removal of K^+ ions from $KFeO_2$ is accompanied by a hydrolization process that is fairly facile in the looser cristobalite structure. $KFeO_2$ can thus be wholly broken down in water or in moisture.

3. Rate of Potassium Leaching from Potassium Ferrite

The leaching process for each of the samples, which were crushed and sieved to 20–40 mesh, 100–120 mesh, and <200 mesh, respectively, has been studied over the temperature range 27–90°C. As expected, the removal of potassium ion from $KFeO_2$ is very rapid in the initial soaking period at each temperature; a dissolution balance is reached in roughly 1 hr. The higher the temperature of the water, the more rapidly the potassium dissolves out. After a near-equilibrium state is reached, the remaining potassium, which may be attributed to adsorption of amorphous Fe_2O_3, is less than 5 wt%, which implies that potassium ferrite of the $KFeO_2$ type no longer exists. For potassium ferrite of the $K_{1+x}Fe_{11}O_{17}$ type, the leaching process at such different temperatures as 27, 50, 70, and 90°C follows a same trend. The leaching rate of potassium is much lower than that of $KFeO_2$; only 20–30% of the potassium has been lost. The leaching rate is slightly faster at higher water temperatures and increases with the reduction of the crushed sample size.

We have presented (*18*) a kinetic equation for the leaching process of potassium in an industrial spherical fused-iron catalyst for ammonia synthesis, as shown by

$$\frac{dy}{dt} = k\frac{c - y}{y}, \qquad (1)$$

where the integrated form is

$$c \ln(c - y) + y = -kt + c \ln c, \qquad (2)$$

where k is a rate constant, t is the time, y is the amount of K_2O leached out per unit weight of catalyst with respect to t, and c is the highest amount of K_2O that can be leached out per unit weight of catalyst.

The above equations successfully describe the leaching process of potassium from the $K_{1+x}Fe_{11}O_{17}$ series. When c was equated with the quantities of K_2O to be dissolved out in 48 hr per gram of each sample into water at 90°C and when we set $w \equiv c \ln(c - y) + y$, straight lines of w vs t were obtained, in which intercept (b) (Table II, Column 4) is $c \ln c$ and the slope (k) is the rate constant (Column 3). A comparison of the value $c \ln c$ assumed (Column 6) with

TABLE II

TEMPERATURE DEPENDENCE OF LEACHING RATE CONSTANT CORRESPONDING TO SAMPLES OF THE $K_{1+x}Fe_{11}O_{17}$ SERIES

Sample	T (°C)	k	b	c (mg/g)	$c \ln c$	E (KJ/mol)
$K_2Fe_{12}O_{19}$	27	0.42	89.1	27.1	89.2	24.5
	50	0.85	89.1			
	70	1.41	89.1			
	90	2.31	89.2			
$K_2Fe_{14}O_{22}$	27	0.38	74.6	23.6	74.6	25.1
	50	0.77	74.6			
	70	1.31	74.6			
	90	2.14	74.7			
$K_2Fe_{22}O_{34}$	27	0.25	45.8	16.4	45.9	26.6
	50	0.54	45.9			
	70	0.95	45.9			
	90	1.61	45.8			

Note. The size of samples is 100–120 mesh.

the value b obtained from the intercept shows that the relative deviations remain below 1% in the temperature range 27–90°C. These results show that the kinetic equation can fit the leaching process of $K_{1+x}Fe_{11}O_{17}$ well and that the values for c are reasonable.

In order to determine the activation energy (E), the Arrhenius equation was used:

$$k = k_0 \exp(-E/RT). \quad (3)$$

The temperature dependence of the rate constants is shown in Fig. 7. The activation energies obtained from the slopes of the lines are all within the scope of diffusion as expected (see Table II), and they are in agreement with those reported in Refs. (*12–13, 19*). The rate constant decreased and the activation energy increased with a reduction in the K/Fe ratio. These results confirm that the leaching process of $K_{1+x}Fe_{11}O_{17}$ involves a slow diffusion process of potassium ion.

It is significant that if one plots c (the highest leachable amount of K_2O) versus x in $K_{1+x}Fe_{11}O_{17}$ and ln y versus $1/T$ (T is Kelvin temperature) when y is small, two straight lines are obtained. Such a result bears some analogy to electronic conductivity of $K_{1+x}Fe_{11}O_{17}$ as a function of the potassium excess x and as a function of temperature, described in Ref. (*11*), where two nearly straight lines were also presented. This analogy implies that there is some unknown relationship between the removal of K^+ caused by water and the electronic conductivity produced by the mobile species in $K_{1+x}Fe_{11}O_{17}$ samples.

4. The Existence of Potash in the Unreduced Iron Catalyst for Ammonia Synthesis

In order to follow the fusion process of the typical commercial catalyst for ammonia synthesis, sample F was investigated. Purified magnetite rather than α-Fe_2O_3 was used as the starting material and the fusion temperature was increased to 1550°C. It was found that the calcined product consisted of Fe_3O_4 and of potassium ferrite of the $K_{1+x}Fe_{11}O_{17}$ type (see Fig. 8). However, when magnetite containing 5.6 wt% K_2O (with a proper amount of iron powder) was fused at over 1600°C in an electric-resistance furnace for about 1 hr and the fused mass was cooled in air, the XRD analysis showed that the

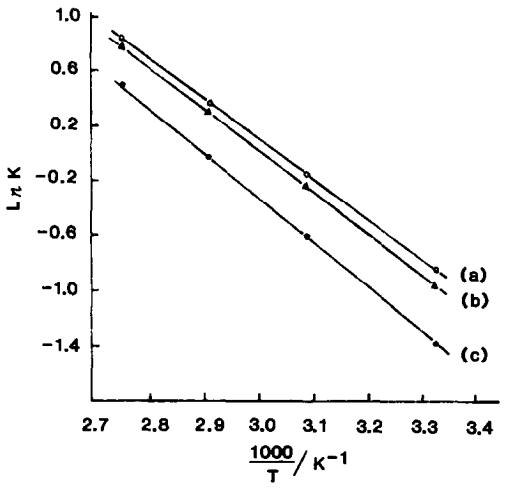

FIG. 7. Plots of ln k versus $1/T$: (a) $K_2Fe_{12}O_{19}$, (b) $K_2Fe_{14}O_{22}$, (c) $K_2Fe_{22}O_{34}$.

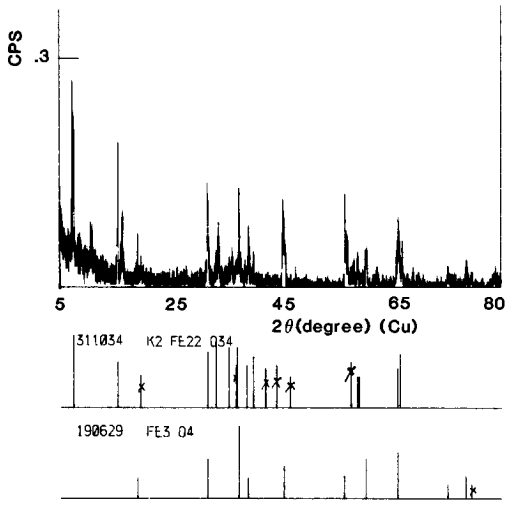

FIG. 8. X-ray diffraction diagram of sample F.

product consisted of three phases: magnetite (Fe_3O_4), Wüstite ($Fe_{1-x}O$), and potassium ferrite of the $KFeO_2$ type (see Fig. 9). The problem now arises as to which type of potassium ferrites might exist in the unreduced iron catalyst for ammonia synthesis. Since the potassium promoter is usually below 2 wt% in the current industrial catalyst, difficulty is encountered in examining its form in the catalyst. From the present results we believe that its form largely depends on the preparation conditions. As a general rule, potassium ion has a stronger tendency to segregate out from the spinel phase of Fe_3O_4. It would seem likely, however, that the potassium ferrite of the $K_{1+x}Fe_{11}O_{17}$ type is preferentially formed within Fe_3O_4, because the spinel structure of magnetite is very similar to that of $K_{1+x}Fe_{11}O_{17}$ with spinel blocks, and the small potassium content in the catalyst conforms to the composition of $K_{1+x}Fe_{11}O_{17}$. In addition, rapid quenching in air or in water in place of slow annealing during preparation of the catalyst leads to rapid cooling of the fused mass. The process favors freezing out of $K_{1+x}Fe_{11}O_{17}$ in the catalyst (*20*). Therefore, these two types of potassium ferrite might coexist in the catalyst in a certain ratio. It could be expected that $KFeO_2$ occurs as a separate phase together with K_2O, $KAlO_2$, Wüstite, etc. at the boundaries of crystal grains of magnetite, but $K_{1+x}Fe_{11}O_{17}$ would be expected to form mainly a solid solution with magnetite.

The question arises whether all of the potash in the fused iron catalyst can be leached out. Kobayashi and Uchida (*7*, *8*) introduced the concept of water-insoluble potash and indicated that the activity of the catalyst for ammonia synthesis largely depends on the potash content. In our previous work (*18*), it was found that even if the catalyst was ground to <200 mesh and soaked in water at 70°C for 24 hr or boiled for 4 hr, it seemed impossible to extract the last remnant of potassium, which is around 0.4 wt% in the catalyst. This verifies that some water-insoluble potash does exist in the fused iron catalyst for ammonia synthesis. If so, we deduce that the insoluble potash should be attributed to potassium ferrite of the $K_{1+x}Fe_{11}O_{17}$ type but not to other types of K compound. This results from the fact that removal of potassium from $K_{1+x}Fe_{11}O_{17}$ is not easy because of the highly dispersive distribution of $K_{1+x}Fe_{11}O_{17}$ within the magnetite grains. Conversely, because other types of potash occur in the boundaries among crystal grains, they are easily hydrolyzed by water.

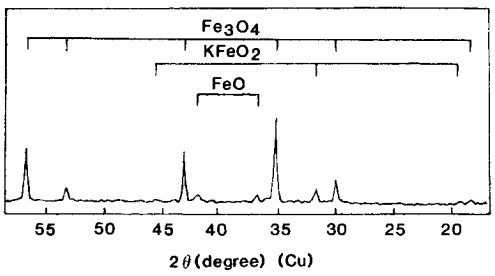

FIG. 9. X-ray diffraction diagram of the magnetite containing 5.6% K_2O after fusion.

Krabetz and Peters (*21*) studied the water-insoluble potassium dependence on the cooling rate during preparation of the catalyst. They found that samples cooled more rapidly contain a greater proportion of the water-insoluble potassium before reduction, a higher potassium concentration on the surface, and a greater free-iron surface area after reduction than those of samples cooled slowly. On the basis of the above discussion, their conclusion appears to be easily explained.

Another question that arises is this: Which potash, soluble or insoluble, does the catalytic activity mainly depend on? In fact, potassium ion in various phases of the unreduced catalyst will redistribute itself and segregate at the surface during the reduction process. Therefore, the form of potassium existing before reduction will be closely related to the surface state of the catalyst after reduction. It seems that the excessive soluble potash massing within boundaries of the unreduced catalyst, such as K_2O, KOH, $KFeO_2$, $KAlO_2$, K_2CO_3, etc., may obstruct some pores and channels and close these to the passage of gases, as well as interfering with the role of the active centers of α-Fe after reduction. Consequently, even if K compounds are partly leached out by water, the catalytic activity will not fall off but may even rise to some extent (*9*). In this connection one should note Paál's investigation (*1*) that a medium surface concentration of K in the adlayer of the working catalyst surface, of roughly 10^{14} K atoms/cm^2 (equivalent to 0.2% of the K_2O content in weight in the current industrial catalyst) optimized catalytic activity. This quantity is close to the figure of 0.4 wt% of insoluble potash, as reported in Ref. (*7*). This rough equality supports the suggestion that the insoluble potash contributes most to the catalytic activity. However, early work on the promoter also showed that the role of the soluble potash cannot be completely ignored (*18, 22*). In a patent (*23*), for example, a catalyst was reported which was prepared by impregnating a prereduced iron catalyst containing 0–0.5 wt% K_2O and suitable amounts of other promoters, in KOH or alkali metal solution. The relative activity of the catalyst for ammonia synthesis was thereby increased by 15–25%. The role of potassium promoter decisively depends on its state and on the sites it occupies after reduction where it can participate in the catalytic activity, rather than on its solubility in water before reduction. From Paál's conclusion, an adlayer with a well-distributed and medium coverage of K should be of greatest benefit to the catalytic activity under real working conditions. The insoluble potash usually exists within the magnetic grains; therefore, after reduction of the catalyst the potassium ions can distribute themselves uniformly and thereby decrease the electron-escaping work function of α-Fe. Naturally, when the soluble potash is introduced into the available site of the reduced catalyst, it will equally promote the activity of α-Fe.

Acknowledgments

We gratefully acknowledge the support of this work by the National Nature Science Foundation Committee of the People's Republic of China.

References

1. Z. Paál, G. Ertl, and S. B. Lee, *Appl. Surf. Sci.* **8,** 231 (1981).
2. H. Topsøe, J. A. Dumesic, and M. Boudart, *J. Catal.* **28,** 477 (1973).
3. H. Ludwiczek and A. Preisinger, *J. Catal.* **51,** 326 (1978).
4. A. Nielsen, "An Investigation on Promoted Iron Catalysts for the Synthesis of Ammonia," 3rd ed., p. 201, Jul. Gjellerups, Copenhagen (1968).
5. N. D. Spencer, R. C. Schoonmaker, and G. A. Somorjai, *J. Catal.* **74,** 129 (1982).
6. G. Ertl and N. Thiele, *Appl. Surf. Sci.* **3,** 99 (1979).
7. H. Kobayashi and O. Nishijima, *J. Chem. Soc. Japan Ind. Chem. Sect.* **57,** 189 (1954).
8. H. Uchida and N. Todo, *Bull. Chem. Soc. Japan* **27**(9), 585 (1954).
9. Wang Wen-Xiang and Li Fan, *Appl. Catal.* **55,** 33–46 (1989).

10. Z. TOMKOWICZ AND A. SZYTUKA, *Phys. Chem. Solids* **38,** 1117 (1977).
11. G. J. DUDLEY, B. C. H. STEELE, AND A. T. HOWE, *J. Solid State Chem.* **18**(2), 141 (1976).
12. G. J. DUDLEY AND B. C. H. STEELE, *J. Solid State Chem.* **21**(1), 1 (1977).
13. T. TAKAHASHI AND K. KUWABARA, *J. Solid State Chem.* **29**(1), 27 (1979).
14. (*a*) PDF (Inorg. 26–1319) by JCPDS (1983); (*b*) PDF (Inorg. 25–651) by JCPDS (1983).
15. T. ICHIDA AND T. SHINJO, *J. Phys. Soc. Japan* **29,** 1109 (1970).
16. T. F. W. BARTH, *J. Chem. Phys.* **3,** 323 (1935).
17. T. A. HOWE AND G. J. DUDLEY, *J. Solid State Chem.* **18**(2), 149 (1976).
18. GUO YI-QUN AND WANG WEN-XIANG, *J. Catal. (China)* **4**(3), 202 (1983). CA: 99, 182197u.
19. K. O. HEVER, *J. Electrochem. Soc.* **115**(8), 826 (1968).
20. Y. OTSUBO AND K. YAMAGUCHI, *J. Chem. Soc. Japan* **82**(6), 676–689 (1961).
21. R. KRABETZ AND CL. PETERS, *Angew. Chem. Int. Ed. Eng.* **4,** 341 (1965).
22. C. BOKHOVEN, C. VAN HEERDEN, R. WESTRIK, AND P. ZWEITERING, *in* "Catalysis" (P. H. Emmett, Ed.), Vol. 3, p. 335, Reinhold, New York (1955).
23. K. ZH. YU, K. F. LI, AND J. H. LI, PRC Patent CN85100601A (1985).
24. G. W. SIMMONS AND H. LEIDHEISER, JR., *in* "Applications on Mössbauer Spectroscopy" (R. L. Cohen, Eds.), Vol. I, p. 92, Academic Press, New York/San Francisco/London (1976).